RSC Advances

ROYAL SOCIETY OF CHEMISTRY

www.rsc.org/advances

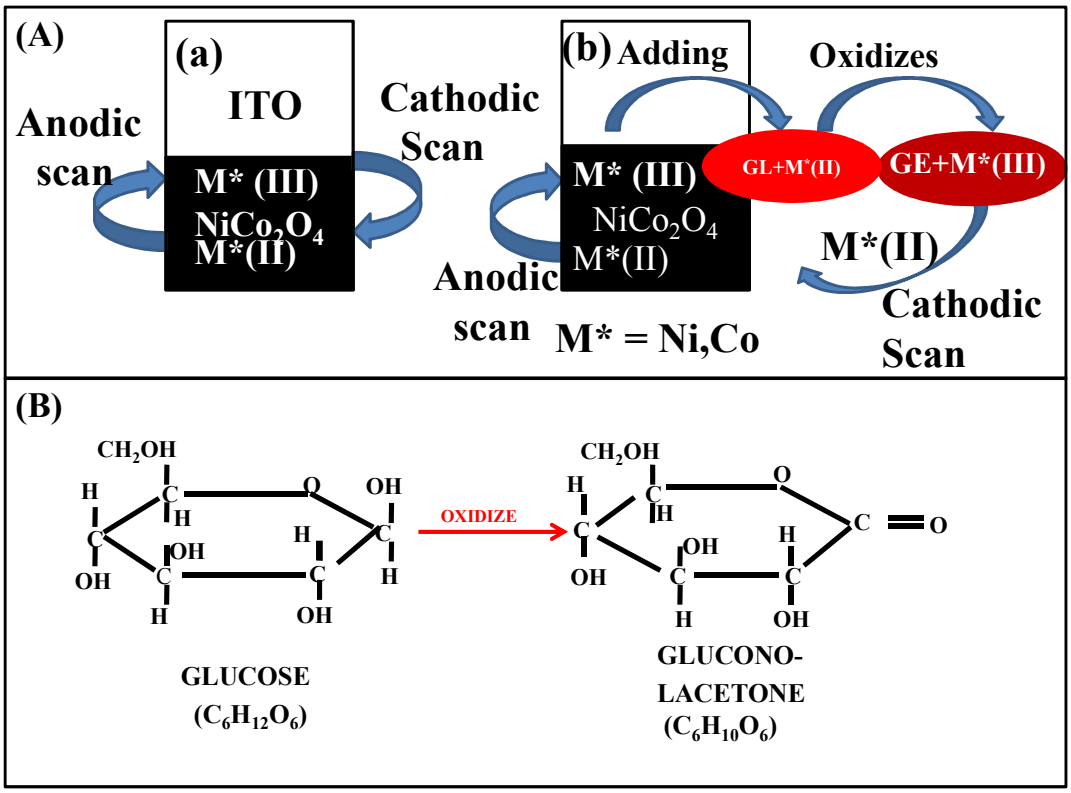

TOC: Non-enzymatic glucose sensing properties of the $NiCo_2O_4$ nanosheets are studied. $NiCo_2O_4$ nanosheets show linear response with respect to the change in glucose concentration varying from 5 to 65 μM and exhibit the sensitivity value of 6.69 $\mu A \mu M^{-1} cm^{-2}$ with a LOD value of 0.38 μM.

Electrodeposited Spinel $NiCo_2O_4$ Nanosheet Arrays for Glucose Sensing Application

Kusha Kumar Naik, Suresh Kumar, Chandra Sekhar Rout *

School of Basic Sciences, Indian Institute of Technology, Bhubaneswar751013, Odisha India

Abstract: We report the growth of $NiCo_2O_4$ nanosheet arrays on a conducting substrate by a simple and highly reproducible electrodeposition method. Non-enzymatic glucose sensing properties of the as-prepared nanosheets are studied. $NiCo_2O_4$ nanosheets show linear response with respect to the change in glucose concentration varying from 5 to 65 μM and exhibit the sensitivity value of 6.69 $\mu A \mu M^{-1} cm^{-2}$ with a LOD value of 0.38 μM. It is proposed that nanosheets are advantageous for glucose sensing applications because of their large surface area with enormous active edges and superior electrochemical properties providing efficient transport pathways for both electrons and ions.

Keywords: Layered materials, Spinel, Nanosheet, Electrodeposition, Glucose sensor

***Corresponding author.** Tel.: +91674-2576092

E-mail address: csrout@iitbbs.ac.in (Dr. C.S. Rout)

1. Introduction

Over the past decade, development of non-enzymatic electrochemical glucose sensors have risen at a considerable rate due to its easy fabrication, cost effective, high sensitivity, fast and accurate measurements. Determination of glucose concentration are not only relevant for use in blood sugar monitoring of many diseases like diabetes, cardiovascular disease and endocrine metabolic disorder but also in the food industry, biotechnology, clinical laboratories and bio-processing.[1] The rising demand for glucose sensors with high sensitivity and reliability, fast response and selectivity have driven tremendous research efforts for decades.[2] To succeed on the fabrication of a high performance glucose sensor, nanostructure metals, metal oxides, chalcogenides and carbon nanomaterials with high surface to volume ratio have been extensively used.[3–6] Furthermore, thin film nanosheets nanomaterials can be used to incorporate the activity of analyte within its local nano-to-micro-scale environment, thereby enhancing the electron transfer between the analyte and the electrode with superior electrochemical properties.

Mixed transition metal oxides (MTMOs), typically ternary metal oxides with two different metal cations, have received an upsurge of interest in recent years due to their promising roles. Spinel $NiCo_2O_4$ is a MTMOs, has received growing attention due to its technological applications in the field of supercapacitor,[7–9] lithium ion batteries,[10] and electrocatalyst,[11] arising from its superior electrochemical properties compared to its binary counterparts and other transition metal oxides. $NiCo_2O_4$ exhibits an inverse spinal structure with Ni cations occupying the octahedral sites while Co cations are evenly distributed to both octahedral and tetrahedral sites.[12] It possesses much better electronic conductivity which is beneficial for fast electron transfer between electrode and electrolyte and the excellent performance can be attributed due to high redox reactions of the cobalt and nickel ions.[11,13,14] The $NiCo_2O_4$

nanostructures greatly improve the performance in electrochemical applications by offering a high specific surface area, short diffusion path for ions or electrons, and efficient channels for mass transport.[15]

Biosensors based on different methods of fabrication have been reported in recent years. Depending on the various properties and phenomena of the detector and techniques used biosensors can be classified into optical biosensors, electrochemical biosensors, electrical biosensors, vibrational biosensors and mechanical biosensors. Among the various biosensors, electrochemical based biosensors involve simple fabrication processes and mechanisim, easier operation, fast response time, low detection limit and posess high stability.[16–18]

Indium tin Oxide (ITO) is transparent and conductive substrates provides the way of excellent electron transfer between the deposited nanostructure and ITO substrates and it provide a reliable platform for the fabrication of biosensor. The glucose immobilized on ITO surfaces are considered to be adsorptions, which contain the carboxylic acid groups or other related functional groups form spontaneous linkages with the ITO surfaces to form stable assemblies.[19–21]

Continuing with the glucose sensor report, Wang *et al.* reported nickel-cobalt nanostructures (Ni-Co NSs) electrodeposited on reduced graphene oxide (RGO)-modified glassy carbon electrode (GCE) for glucose sensor applications.[22] Similarly Dong *et al.* reported glucose sensing properties of Co_3O_4 nanowires on three-dimensional graphene foam grown by chemical vapour deposition .[23] Li *et al.* reported uniform growth of large-area 3D β-$Ni(OH)_2$ and NiO nanowalls on a variety of rigid and flexible substrates for electrochemical glucose sensor applications.[24]

Herein, we report the growth of $NiCo_2O_4$ nanosheet arrays on indium tin oxide (ITO) coated glass substrate by electrodeposition method. The electrochemical sensing behaviour of the nanosheets towards glucose molecule is studied. The developed $NiCo_2O_4$ nanosheets based

glucose sensor shows linear response towards varying glucose concentration in a range from 5 to 65 μM with a sensitivity value of 6.69 $\mu A \mu M^{-1} cm^{-2}$, LOD (Limit of Detection) value of 0.38 μM and LOQ (liquid of quantification) is 1.27 μM. It has been proposed that the $NiCo_2O_4$ nanosheets are advantageous for glucose sensing applications because of its efficient transport pathways for both electrons and ions.[25,26]

2. Experimental Section

2.1 Material Preparation

The electrodeposition of $NiCo_2O_4$ has been carried out by electrochemical chrono-amperometric technique in a glass cell with three electrodes configuration. In the first step, 0.01 M nickel nitrate hexahydrate and 0.02 M cobalt nitrate hexahydrate were dissolved in 10 ml of de-ionized water (DI). After complete dissolution, 0.01 M of Potassium chloride (KCl) was mixed as supporting electrolyte. The three electrodes of the electrodeposition set-up consist of Pt as counter electrode, Ag/AgCl as reference electrode and ITO/glass as working electrode. The portion of the working electrode where the $NiCo_2O_4$ needs to be deposited was dipped in to the solution and rest part of the ITO was kept in air. In the second step, -1.1 V potential was applied to the electrode for 180 s and the temperature of the solution was maintained at 70 ºC by a hot plate with continuous magnetic stirring. At high temperature with applied potential, the dissolved Ni and Co ions attract to each other by a driving force and nucleate to form $NiCo_2O_4$ seed layers and further growth during the electrodeposition process lead to the formation of nanosheet arrays. In the next step, the as-prepared $NiCo_2O_4$ nanosheet arrays on ITO/glass was dried at room temperature overnight followed by calcination at 500 ºC for 6 hour. At 500 ºC, formation of black coloured and pure phase of $NiCo_2O_4$ nanosheets took place.

2.2. Material Characterization

The crystallinity of the as-synthesized material was characterized by X-ray diffraction (XRD) patterns of Bruker D8 Advanced diffractometer using Cu-Kα radiation (λ = 1.54184 Å). Morphology and composition of the as-prepared samples were examined by FESEM ((MERLIN Compact with GEMINI I electron column, Zeiss Pvt. Ltd., Germany) equipped with energy dispersive X-ray spectroscopy (EDAX).

2.3. Electrochemical Glucose sensing Measurements

Cyclic voltammetery (CV) and Chrono-amperometry (CA) experiments were performed by using a PG262A potentiostat/galvanostat (Technoscience Ltd., Bangalore, India). All the electrochemical experiments were performed in a three electrode glass cell containing 0.1 M NaOH aqueous solution as the electrolyte. The $NiCo_2O_4$ nanosheet arrays grown on ITO/glass were used as the working electrode; Ag/AgCl and platinum wire were used as reference and counter electrode respectively. For CV measurements, all the electrodes were dipped in 6 ml of NaOH solution and the potential window in the range of -0.3 to 0.9 V was selected to observe the oxidation and reduction peak positions. Similarly, for CA measurements, a potential value of 0.4 V was applied in a glass cell containg 140 ml of NaOH aquous solution and change in current with respect to the glucose concentrations have been measured after an interval of time of 100 s.

3. Results and discussion

Morphology of the as-synthesized $NiCo_2O_4$ nanosheets was observed by FESEM depicted in Fig. 1a and b. The electrodeposited nanosheets are homogeneous, uniform and well populated though out the surface of ITO which can be clearly seen in the low magnification FESEM image as shown in Fig. 1a. The lateral length of the nanosheets were 2-3 μm range and a thickness ~30-50 nm.

The crystalline phase of the annealed black thin film samples were identified by XRD. As shown in Fig. 1c, all the characteristic diffraction peaks, (111), (220), (311), (222), (400), (422), (511) and (440) can be indexed to cubic $NiCo_2O_4$ crystal structure (JCPDS card No. 20-0781) having lattice parameter a=b=c= 8.11 Å. No other impurity peaks were observed suggesting that the synthesized material is of high purity with good crystalline.[27] The surface compositions of $NiCo_2O_4$ nanosheets were determined by EDAX, confirming the presence of Ni, Co, and O atoms Fig. 1d. The elemental mapping of the $NiCo_2O_4$ nanosheets indicated the uniform distribution of the individual atoms (Ni, Co, and O) throughout the as-grown sample Fig. 2. Atomic ratio of Ni, Co and O was estimated to be nearly 1:2:4 confirming the formation of pure $NiCo_2O_4$ phase.

The electrocatalytic property of the $NiCo_2O_4$ film was first asserted by CV measurements taking a potential range from -0.3 to 0.9 V in 0.1 M NaOH solution at a scan rate of 40 mVs^{-1}. The CVs of $NiCo_2O_4$ nanosheets without glucose and in different concentrations of glucose solution (From 100-1000 μM with successive increase in concentration by 100 μM) are depicted in Fig. 3a. In anodic scan, a broad oxidation peak in the 0.4-0.9 V range was observed and the amplitude of the oxidation peak increased and reduction peak decreased with each addition of glucose concentration in the solution as shown in Fig. 3a. This change in the peak current sucessively suggested that the electrodeposited $NiCo_2O_4$ nanosheet is a stable and good electro catalytic material suitable for glucose sensing applications.[23,28–31]

The mechanism of increase in peak current is shown in Fig. 4(A), and it can be understood as follows:

$$NiCo_2O_4 + OH^- + H_2O \leftrightarrow NiOOH + 2CoOOH + e^- \quad \text{----------(1)}$$

$$CoOOH + OH^- \leftrightarrow CoO_2 + H_2O + e^- \quad \text{----------(2)}$$

$Ni\ (II) + Co\ (II) \rightarrow Ni\ (III) + Co\ (III) + 2e^{-}$----------(3)

Glucose ($C_6H_{12}O_6$) → Gluconolactone ($C_6H_{10}O_6$) + $2H^{+}$ + $2e^{-}$----------(4)

During the anodic scan, Ni (II) and Co (II) species present in the dissolved NiOOH and CoOOH compounds oxidise to Ni (III) and Co (III) species in the appied potential range by releasing two electrons, (Eq. 3). when we droped the glucose molecules , the glucose molecule (GL) dissociate and converted to gluconolactone (GE) by giving up two electrones into the solution, (Eq. 4, Fig. 4b). The oxidation of Ni and Co ions and glucose molecules occure simultaneouly in the same potential range but the rate of oxidations of Ni and Co ions present on the electrode surface determine the rate of detection of glucose molecules. Thus the detection of glucose molecule is the intrinsic electrochemical activity of the material and the rate of detection can be enhanced by the engineering the morphology of the materials and controling the other parameters like pH,.molarity of aquous solution and the substrate.[28,32–34]

In cathodic scan, the oxidised Ni (III) , Co (III) species reduce to Ni (II) and Co (II) ions by accepting the electrons and returns to its original state (Eq. 5).[27,35–37] Thus oxidation and reduction are observed in each addition of glucose molecules in the elctrolyte. The anodic peak current increases periodically by increasing glucose concentration due to release of more number of electrons. Again the high affinity of glucose to glucanolactone can be attributed to $NiCo_2O_4$ due to its biocompatibility, large surface area, active edges and high electron communication capability. [38–41] Fig. 3b shows linear response of oxidation peak with correlation co-efficient R^2=0.99. This means that the $NiCo_2O_4$ nanosheets prepared by us exhibit uniform response of glucose molecules and show good electro catalytic behaviour.

Fig. 3c shows CVs of $NiCo_2O_4$ nanosheets electrode at different scan rates in the presence of 100 μM glucose concentration in the solution. The obtained result showed that both the oxidation and reduction peak current increase linearly with increasing scan rates because

by increasing scan rate, electrons transfer between the surface of the electrode and electrolyte increases. A graph of the anodic and cathodic peak current against the square root of the scan rate is shown in Fig. 3d. It exhibits a linear relation demonstrating that the oxidation of glucose at the electrode surface is a diffusion controlled process.[42,43] It can be found that the peak current is proportional to the square root of scan rate, showing a typical diffusion controlled electrochemical behaviour. But the CV remained unchanged at different scan rates which confirmed that the $NiCo_2O_4$ nanosheets are a stable material for glucose sensing.

Amperometric measurement was recorded to estimate the detection limit and the sensitivity value of $NiCo_2O_4$ nanosheet electrode at different glucose concentrations. The measurements have been carried out at 0.4 V potential under the vigorous stirring of the solution at 1100 rpm. When 5 μM of glucose molecules added into the 140 ml of NaOH aqueous solution the current rose steeply to reach a stable value with a response time of 26 s. The current value increased successively by periodic addition of 5 μM of glucose molecules into the solution with a time interval of 100 s (Fig. 5a). The sensitivity and linear range of detection can be found by taking the consideration of calibration graph which observed that $NiCo_2O_4$ nanosheets show linear response value from 5 to 65 μM glucose concentrations with the sensitivity value of 6.69 $\mu A \mu M^{-1} cm^{-2}$. The limit of detection (LOD) and limit of quantification (LOQ) of the amperometric glucose sensor were estimated using the formula in eqn 6 & 7[44]

$$LOD = \frac{3\, s_b}{m} \qquad \text{----------(5)}$$

$$LOQ = \frac{10 s_b}{m} \qquad \text{---- ----------(6)}$$

where s_b is the standard deviation obtained from five measurements of the blank signal (0.00057 mA) and m is the slope value extracted from the calibration plot (0.00446 mA μM^{-1}). Using these data, LOD and LOQ were calculated to be 0.38 μM and 1.27 μM respectively .

One of the most important analytical factors for an amperometric biosensor is the selectivity of the sensor to target analyte. It is well-known that Ascorbic acid (AA) ,uric acid (UA), Lactic acid (LA) and dopamine (DA) are common interfering species during catalytic oxidation of glucose. The interference study has been carried out at 0.4 V potential under the same experimental condition in the glass cell by adding the 5 μM of UA, DA,LA and AA contineously into the solution in the separation of 100 s, Fig. 5c. The present electrode can successfully avoid interferences from UA, DA, LA and AA . Furthermore, we performed the interference test to demonstrate the ability of our sensor to differentiate glucose from fructose, which is isomeric with glucose. To investigate the reproducibility of the $NiCo_2O_4$ nanosheets electrode, seven independently fabricated electrodes were tested for glucose sensing and it showed an acceptable reproducibility with a relative standard deviation of 3.1% for the current determined at a glucose concentration of 5 μM. The stability of the electrode by monitoring the remaining amount of current response after successive cycling of the electrode for 100 circles was examined. It was found that the peak current for glucose oxidation retains 90 % of its initial value. Again, we observed CA experiment in the presence of 100 μM of glucose concentration at 0.4 V potential for 3000 s. The $NiCo_2O_4$ nanosheets showed linear characteristic up to 3000 s Fig. 5e. The synthesized non-enzymatic glucose sensor possesses a low LOD of 0.38 μM and a linear range from 5-65 μM which are excellent for glucose sensors. To check the advantages of $NiCo_2O_4$ nanosheets compared to its binary oxides such as NiO and Cobalt oxide we carried out the glucose sensing performance of the binary oxides prepared by following same electrodeposition method. It is observed that NiO was insensitive to glucose under the same measurement condition used for $NiCo_2O_4$ nanosheets. The glucose sensing performance of

cobalt oxide is shown in Fig. S1. and S2. † Cobalt oxide showed a sensitivity of ~ 3.5 $\mu A \mu M^{-1} cm^{-2}$ with LOD 0.38 µM which is low compared to NiCo2O4 nanosheets.

We have also prepared $NiCo_2O_4$ nanosheet arrays on other conductive substrates such as Ni foam and Ni strip and their glucose sensing properties were studied (See Fig. S4, S5, S6, S7). † Table 1 shows the comparison of the glucose sensing performance of the $NiCo_2O_4$ nanosheet arrays prepared on different substrates. The obtained sensitivity are 0.046 $mA \mu M^{-1} cm^{-2}$ and 0.018 $mA \mu M^{-1} cm^{-2}$ for the $NiCo_2O_4$ nanosheets grown on Ni foam and Ni strip respectively with the response time in the similar range of the $NiCo_2O_4$ nanosheets grown on ITO/glass substrates. Further, the glucose sensing performance of $NiCo_2O_4$ nanosheets are compared with the previous reports on Ni-Co-oxides for glucose sensing applications and our results are comparable to the literature (Table 2).

4. Conclusion

In conclusion, $NiCo_2O_4$ nanosheets were grown on ITO/glass substrate by a simple electrodeposition method. The $NiCo_2O_4$ nanosheets can be readily obtained by making the seed layer and tuning the deposition time with enhanced electrocatalic activity suitable for electrochemical glucose sensing applications. The $NiCo_2O_4$ nanosheets-based glucose sensor exhibited extremely high sensitivity to glucose (6.69 $\mu A \mu M^{-1} cm^{-2}$), a low detection limit of 0.38 µM and good linear range response from 5- 65 µM. Hence the present electrodeposition method for $NiCo_2O_4$ nanosheets growth paves the way for fabricating glucose sensors with low cost, high sensitivity and good detection limit with great potential for industrial mass production.

Acknowledgements

Dr. C.S. Rout would like to thank DST (Government of India) for the Ramanujan fellowship. This work was supported by the DST-SERB Fast-track Young scientist (Grant No. SB/FTP/PS-

065/2013), UGC-UKIERI thematic awards (Grant No. UGC-2013-14/005) and BRNS-DAE, (Grant No. 37(3)/14/48/2014-BRNS/1502).

Reference

1 S. C. Port, N. G. Boyle, W. A. Hsueh, M. J. Quiñones, R. I. Jennrich and M. O. Goodarzi, *Am. J. Epidemiol.* , 2006, **163** , 342–351.

2 M. A. Arnold and G. W. Small, *Anal. Chem.*, 2005, **77**, 5429–5439.

3 E. Katz and I. Willner, *Angew. Chemie Int. Ed.*, 2004, **43**, 6042–6108.

4 N. A. Rakow and K. S. Suslick, *Nature*, 2000, **406**, 710–713.

5 N. L. Rosi and C. A. Mirkin, *Chem. Rev.*, 2005, **105**, 1547–1562.

6 Y. Lin, F. Lu, Y. Tu and Z. Ren, *Nano Lett.*, 2004, **4**, 191–195.

7 X. Lu, X. Huang, S. Xie, T. Zhai, C. Wang, P. Zhang, M. Yu, W. Li, C. Liang and Y. Tong, *J. Mater. Chem.*, 2012, **22**, 13357–13364.

8 Q. Wang, X. Wang, B. Liu, G. Yu, X. Hou, D. Chen and G. Shen, *J. Mater. Chem. A*, 2013, **1**, 2468–2473.

9 X.-Y. Yu, X.-Z. Yao, T. Luo, Y. Jia, J.-H. Liu and X.-J. Huang, *ACS Appl. Mater. Interfaces*, 2014, **6**, 3689–3695.

10 J. Li, S. Xiong, Y. Liu, Z. Ju and Y. Qian, *ACS Appl. Mater. Interfaces*, 2013, **5**, 981–988.

11 L. Qian, L. Gu, L. Yang, H. Yuan and D. Xiao, *Nanoscale*, 2013, **5**, 7388–7396.

12 J. F. Marco, J. R. Gancedo, M. Gracia, J. L. Gautier, E. Ríos and F. J. Berry, *J. Solid State Chem.*, 2000, **153**, 74–81.

13 J. Xiao and S. Yang, *RSC Adv.*, 2011, **1**, 588–595.

14 L. Hu, L. Wu, M. Liao, X. Hu and X. Fang, *Adv. Funct. Mater.*, 2012, **22**, 998–1004.

15 R. Zou, K. Xu, T. Wang, G. He, Q. Liu, X. Liu, Z. Zhang and J. Hu, *J. Mater. Chem. A*, 2013, **1**, 8560–8566.

16 J. R. Askim, M. Mahmoudi and K. S. Suslick, *Chem. Soc. Rev.*, 2013, **42**, 8649–8682.

17 M. S. Artiles, C. S. Rout and T. S. Fisher, *Adv. Drug Deliv. Rev.*, 2011, **63**, 1352–1360.

18 A. Matsumoto and Y. Miyahara, *Nanoscale*, 2013, **5**, 10702–10718.

19 J. Lin, L. Zhang and S. Zhang, *Anal. Biochem.*, 2007, **370**, 180–185.

20 A. Fang, H. Ng, X. Su and S. F. Y. Li, *Langmuir*, 2000, **16**, 5221–5226.

21 A. Fang, H. T. Ng and S. F. Y. Li, *Biosens. Bioelectron.*, 2003, **19**, 43–49.

22 L. Wang, X. Lu, Y. Ye, L. Sun and Y. Song, *Electrochim. Acta*, 2013, **114**, 484–493.

23 X.-C. Dong, H. Xu, X.-W. Wang, Y.-X. Huang, M. B. Chan-Park, H. Zhang, L.-H. Wang, W. Huang and P. Chen, *ACS Nano*, 2012, **6**, 3206–3213.

24 G. Li, X. Wang, L. Liu, R. Liu, F. Shen, Z. Cui, W. Chen and T. Zhang, *Small*, 2015, **11**, 731–739.

25 H. Jiang, J. Ma and C. Li, *Chem. Commun.*, 2012, **48**, 4465–4467.

26 G. Zhang and X. W. (David) Lou, *Adv. Mater.*, 2013, **25**, 976–979.

27 Q. Wang, B. Liu, X. Wang, S. Ran, L. Wang, D. Chen and G. Shen, *J. Mater. Chem.*, 2012, **22**, 21647–21653.

28 C. Guo, Y. Wang, Y. Zhao and C. Xu, *Anal. Methods*, 2013, **5**, 1644–1647.

29 Y. Mu, D. Jia, Y. He, Y. Miao and H.-L. Wu, *Biosens. Bioelectron.*, 2011, **26**, 2948–2952.

30 Y. Ding, Y. Wang, L. Su, M. Bellagamba, H. Zhang and Y. Lei, *Biosens. Bioelectron.*, 2010, **26**, 542–548.

31 C.-W. Kung, C.-Y. Lin, Y.-H. Lai, R. Vittal and K.-C. Ho, *Biosens. Bioelectron.*, 2011, **27**, 125–131.

32 S. K. Arya, S. Saha, J. E. Ramirez-Vick, V. Gupta, S. Bhansali and S. P. Singh, *Anal. Chim. Acta*, 2012, **737**, 1–21.

33 I.-H. Yeo and D. C. Johnson, *J. Electroanal. Chem.*, 2000, **484**, 157–163.

34 C. P. Wilde and M. Zhang, *J. Chem. Soc.{,} Faraday Trans.*, 1993, **89**, 385–389.

35 Y. Li, P. Hasin and Y. Wu, *Adv. Mater.*, 2010, **22**, 1926–1929.

36 Z. Wu, Y. Zhu and X. Ji, *J. Mater. Chem. A*, 2014, **2**, 14759–14772.

37 H. Huo, Y. Zhao and C. Xu, *J. Mater. Chem. A*, 2014, **2**, 15111–15117.

38 W. Liu, C. Lu, K. Liang and B. K. Tay, *J. Mater. Chem. A*, 2014, **2**, 5100–5107.

39 G. Zhang and X. W. (David) Lou, *Sci. Rep.*, 2013, **3**.

40 C. Yuan, J. Li, L. Hou, X. Zhang, L. Shen and X. W. (David) Lou, *Adv. Funct. Mater.*, 2012, **22**, 4592–4597.

41 J. Du, G. Zhou, H. Zhang, C. Cheng, J. Ma, W. Wei, L. Chen and T. Wang, *ACS Appl. Mater. Interfaces*, 2013, **5**, 7405–7409.

42 R. K. Srivastava, S. Srivastava, T. N. Narayanan, B. D. Mahlotra, R. Vajtai, P. M. Ajayan and A. Srivastava, *ACS Nano*, 2012, **6**, 168–175.

43 Y. Zou, L. He, K. Dou, S. Wang, P. Ke and A. Wang, *RSC Adv.*, 2014, **4**, 58349–58356.

44 G. Knobel, K. Calimag-Williams and A. D. Campiglia, *Analyst*, 2012, **137**, 5639–5647.

45. Mushtaque Hussain, Zafar Hussain Ibupoto, Mazhar Ali Abbasi, Xianjie Liu, Omer Nur, and Magnus Willander Sensors (Basel). 2014 , **14,** 5415–5425

Electrode	Sensitivity	Linear range	LOD	Response time
$NiCo_2O_4$/ITO	6.69 $\mu A \mu M^{-1} cm^{-2}$	5-65 µM	0.38 µM	26 s
$NiCo_2O_4$/Ni foam	0.046 $mA \mu M^{-1} cm^{-2}$	5-50 µM	8.5 µM	21s
$NiCo_2O_4$/Ni strip	0.018 $mA \mu M^{-1} cm^{-2}$	5-65 µM	4.6 µM	27 s

Table-1 Comparision of glucose sensing performance of $NiCo_2O_4$ nanosheets prepared on different electrodes.

Electrode	Sensitivity	Linear range	LOD	Response time	Reference
$NiCo_2O_4$ nanoneedles on Ni foam(Enzymatic)	91.34 mV/decade	0.005-15 mM	—	10 s	45
CNT-NiCo-oxide	66.15 $\mu A \mu M^{-1} cm^{-2}$	0.02-12.12 mM	5 µM	—	[22]
$NiCo_2O_4$ nanosheets/ITO	6.69 $\mu A \mu M^{-1} cm^{-2}$	6-65 µM	0.38 µM	26 s	Present work

Table-2 Comparision of glucose sensing performance of $NiCo_2O_4$ nanosheets with reported literature.

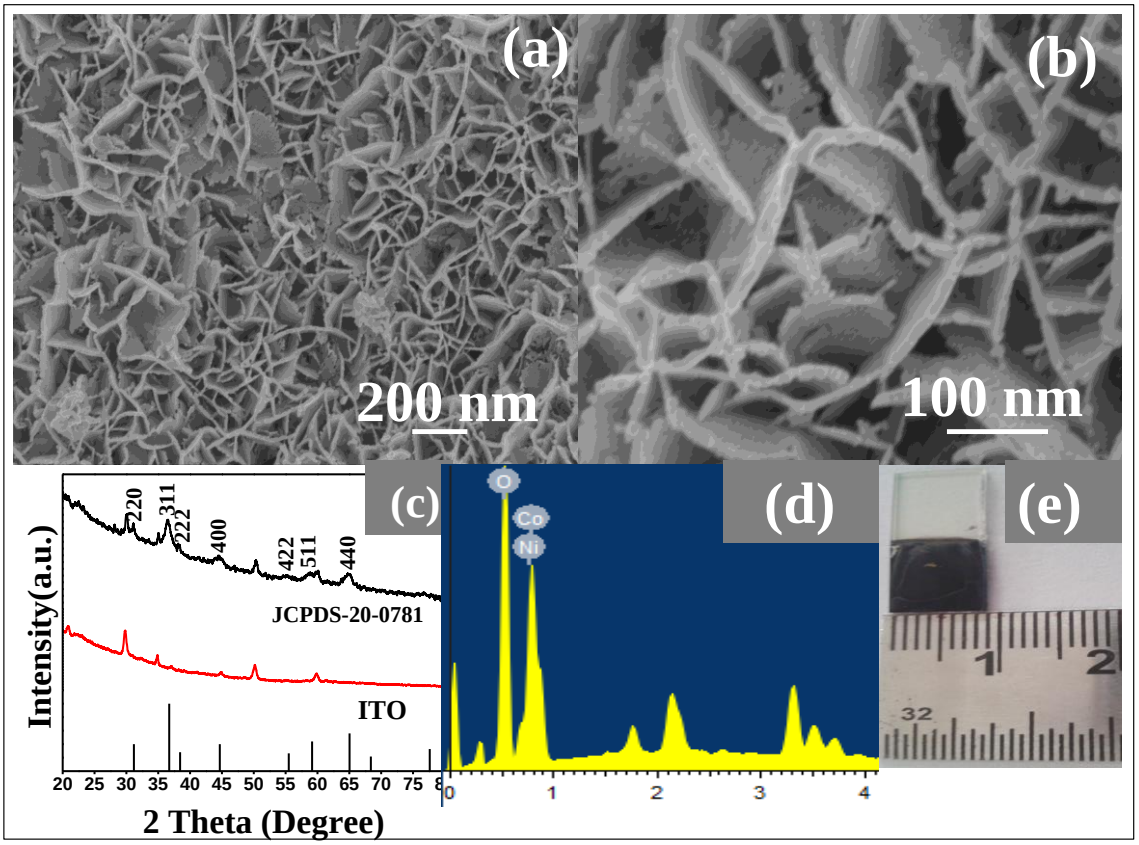

Fig. 1. (a) and (b) Low and high magnification FESEM images of $NiCo_2O_4$ nanosheet arrays grown on ITO coated glass. (c) XRD pattern, (d) EDX spectrograph and (e) photograph of the as-prepared $NiCo_2O_4$ sample.

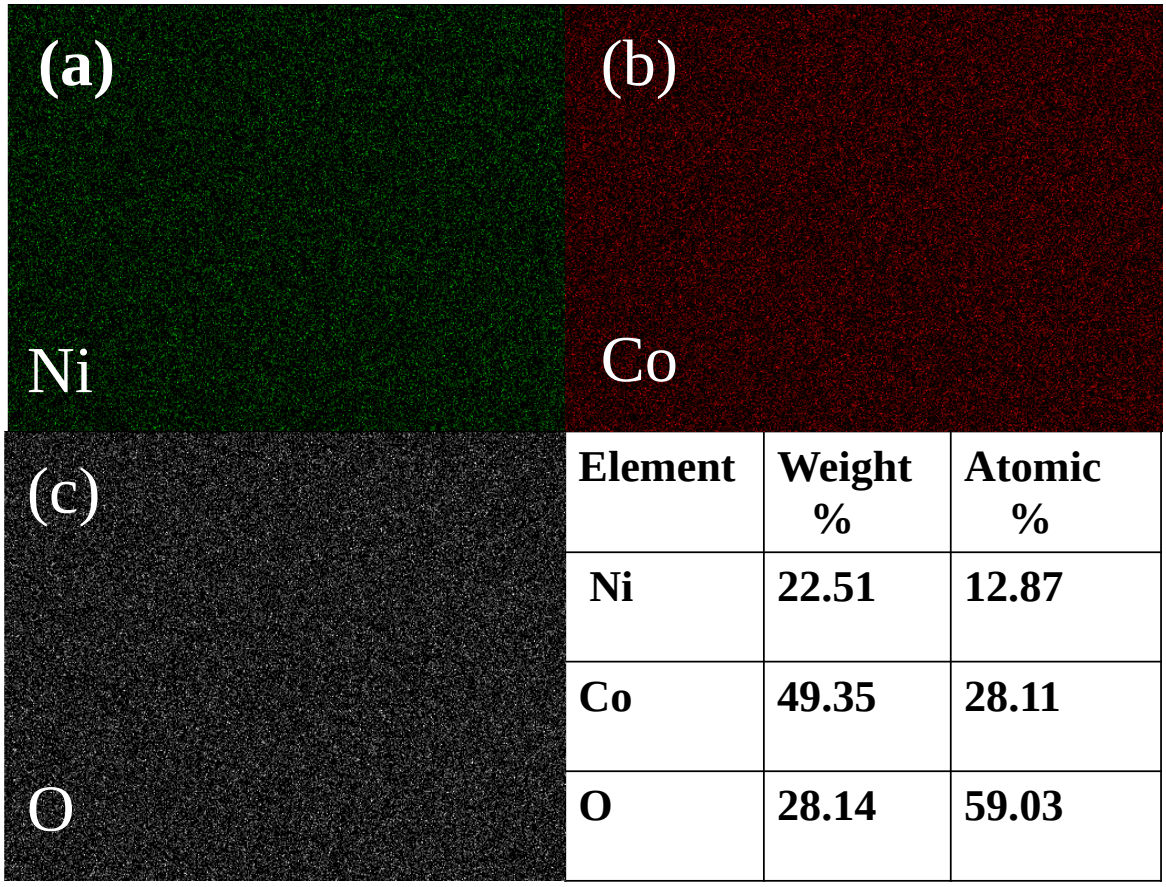

Element	Weight %	Atomic %
Ni	22.51	12.87
Co	49.35	28.11
O	28.14	59.03

Fig. 2. Elemental mapping of the $NiCo_2O_4$ nanosheet arrays: (a) Ni, (b) Co ,and (c) O.

Comparative table showing percentage of the elements

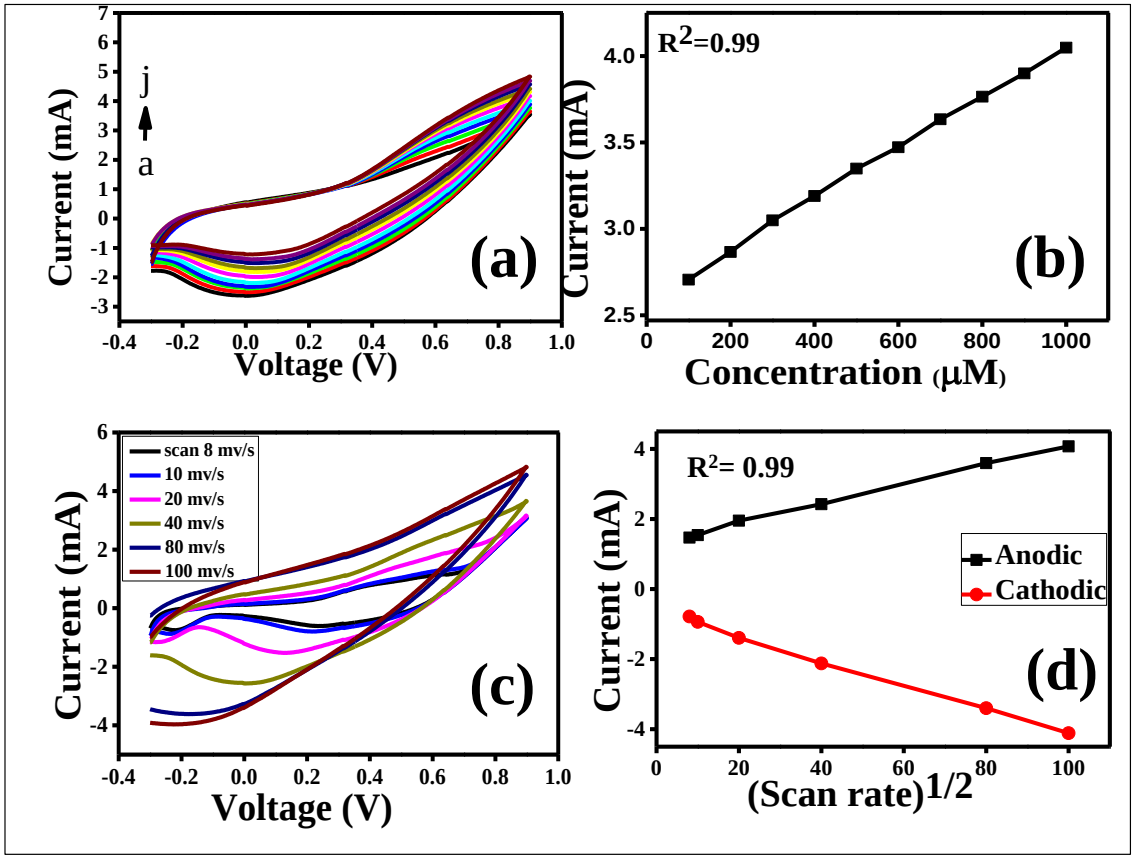

Fig. 3. (a) CVs of $NiCo_2O_4$ electrode at different glucose concentrations: black colour solid line shows the CV without glucose and in (a) 100 μM to (j) 1000 μM glucose in 0.1 M of NaOH. (b) Variation of oxidation peak current at different glucose concentration, (c) CVs in presence of 100 μM glucose at different scan rate, (d) Variation of oxidation and reduction peak current at different scan rate for 100 μM glucose.

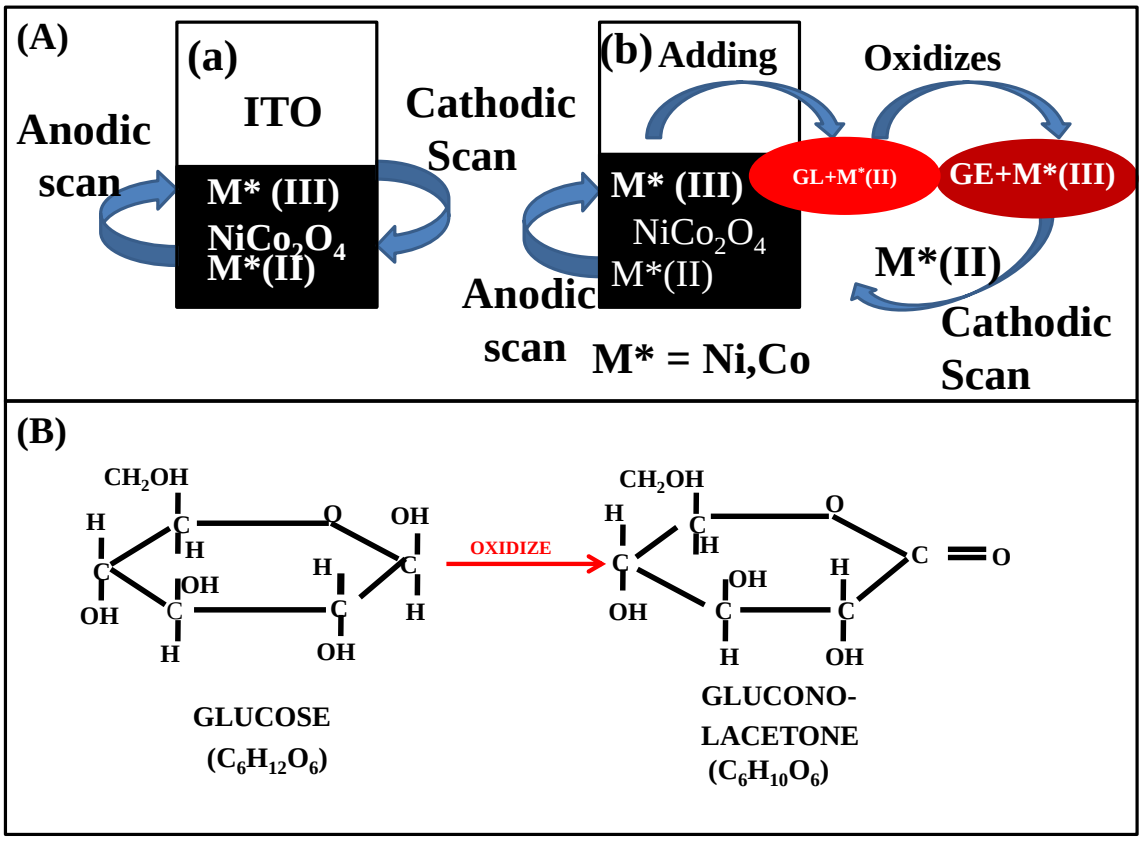

Fig. 4.(A) Mechanism of glucose sensing of the $NiCo_2O_4$ nanosheets: (a) Without glucose and (b) in presence of glucose.(B) shematic diagram of glucose and gluconolactone.

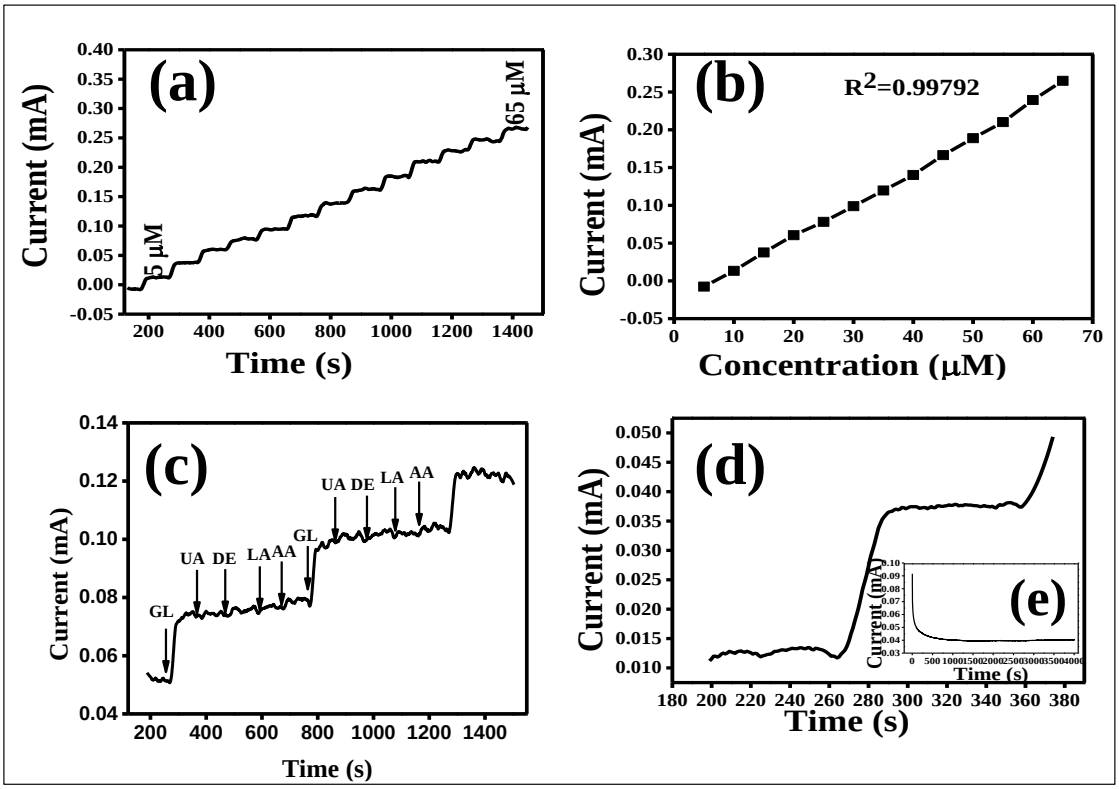

Fig. 5. (a) Current versus time measurement at 0.4 V with successive addition of 5 µM of glucose in 100 s time interval. (b) Dependence on current with respect to the glucose concentration, (c) Interference study, (d) Response time of the sensor to achieve steady-state current, and (e) inset showing stability graph in presence of 100 µM glucose concentration in 0.1 M of NaOH.